Stochastic Analysis of Deep-Submicrometer CMOS Process for Reliable Circuits Designs

Amir Zjajo, *Member, IEEE*, Qin Tang, Michel Berkelaar, *Member, IEEE*, Jose Pineda de Gyvez, *Fellow, IEEE*, Alessandro Di Bucchianico, and Nick van der Meijs, *Member, IEEE*

Abstract—**A time-domain methodology for statistical simulation of nonlinear dynamic integrated circuits with arbitrary excitations is presented. The statistical behavior of the circuits is described as a set of stochastic differential equations rather than estimated by a population of realizations and Gaussian closure approximations are introduced to obtain a closed form of moment equations. Statistical simulation of specific circuits shows that the proposed numerical methods offer accurate and efficient solution of stochastic differentials for variability and noise analysis of integrated circuits.**

Index Terms—**Noise analysis, statistical simulation, stochastic differential equations, variability.**

I. INTRODUCTION

ONE of the most notable features of nanometer-scale CMOS technology is the increasing magnitude of variability of the key parameters affecting performance of integrated circuits [1]. Although scaling made controlling extrinsic variability more complex, nonetheless, the most profound reason for the future increase in parameter variability is that the technology is approaching the regime of fundamental randomness in the behavior of silicon structures where device operation must be described as a stochastic process. Since placement of dopant atoms introduced into silicon crystal is random, the final number and location of atoms in the channel of each transistor is a random variable. As the threshold voltage of the transistor is determined by the number and placement of dopant atoms, it will exhibit a significant variation [2]. This leads to variation in the transistors' circuit-level properties, such as delay and power [3]. Similarly, electric noise due to the trapping and detrapping of electrons in lattice defects may result in large current fluctuations, and those may be different for each device within a circuit. At this scale, a single-dopant atom may change device characteristics, leading to large variations from device to device [4]. As the device gate length approaches the correlation length of the oxide-silicon interface, the intrinsic threshold voltage fluctuations induced by local oxide thickness variation will become significant [2]. Finally, line-edge roughness, i.e., the random variation in the gate length along the width of the channel, will also contribute to the overall variability of gate length [5]. In addition to device variability, which sets the limitations of circuit designs in terms

of accuracy, linearity and timing, existence of electrical noise associated with fundamental processes in integrated-circuit devices represents an elementary limit on the performance of electronic circuits.

Device variability effects and noise limitations are rudimentary issues for the robust circuit design and their evaluation has been subject of numerous studies. Several models have been suggested for device variability [6]–[8] and for noise [9]–[12], and correspondingly, a number of computer-aided design (CAD) tools for statistical circuit simulation [13]–[18] and noise analysis [9], [19], [20]. Monte Carlo analysis is a widespread approach for statistical analysis of circuits affected by technological variations and/or noise simulation in time domain. The Monte Carlo algorithm takes random combinations of values chosen from within the range of each process parameter and repeatedly performs circuit simulations. The result is an ensemble of responses from which the statistical characteristics are estimated. Unfortunately, if the number of iterations for the simulation is not very large, Monte Carlo simulation always underestimates the tolerance window. Accurately determining the bounds on the response requires a large number of simulations, so consequently, the Monte Carlo method becomes very *cpu*-time consuming if the chip becomes large. Other approaches for statistical analysis of variation-affected circuits, such as the one based on the Hermite polynomial chaos [21] or the response surface methodology, are able to perform much faster than a Monte Carlo method at the expense of a design of an experiments preprocessing stage [22]. The noise performance of a circuit can be analyzed in terms of the small-signal equivalent circuits by considering each of the uncorrelated noise sources in turn and separately computing their contribution at the output. Unfortunately, this method is only applicable to circuits with fixed operating points and is not appropriate for noise simulation of circuits with changing bias conditions. In this paper, we propose a direct approach to statistical simulation, based on solving the equations (necessarily stochastic) which describe the statistical behavior of the circuit, rather than estimating it by a population of realizations. The circuits are described as a set of stochastic differential equations and Gaussian closure approximations are introduced to obtain a closed form of moment equations. Even if a random variable is not strictly Gaussian, a second-order probabilistic characterization yields sufficient information for most practical problems. The method employed is an enhanced version of [18] with an extension for transient analysis. Additionally, we suggest numerical methods for the efficient solution of stochastic differentials for noise analysis.

This paper treats static manufacturing variability and dynamic statistical fluctuation separately, and is organized as follows: Section II focuses on the process variability and noise models. Process variations are modeled as a wide-sense stationary process and Section III discusses a solution of a system of stochastic differential equations for such process. On the other hand, circuit noise is a nonstationary process, formulated as a system of mixed stochastic algebraic and Ito stochastic differential equations. In Section IV, an accurate and efficient solution of such a system based on a low rank version of a Lyapunov equations approach is presented. In Section V accuracy considerations of the stochastic state space models, e.g., voltage nodes and current brunches, are discussed. In Section VI, experimental results obtained on two prototypes, a continuous-time biquad filter and a discrete-time variable gain amplifier, both fabricated in standard 65-nm CMOS are presented. Finally, Section VII provides a summary and the main conclusions.

II. PROCESS VARIABILITY AND NOISE MODELS

A. Modeling Process Variability

The availability of large data sets of process parameters obtained through parameter extraction allows the study and modeling of the variation and correlation between process parameters, which is of crucial importance to obtain realistic values of the modeled circuit unknowns. The fundamental notion for the study of spatial statistics is that of stochastic (random) process defined as a collection of random variables on a set of temporal or spatial locations. Generally, a second-order stationary [wide sense stationary (WSS)] process model is employed, but other more strict criteria of stationarity are possible. This model implies that the mean is constant and the covariance only depends on the separation between any two points. In a second-order stationary process only the first and second moments of the process remain invariant. The covariance and correlation functions capture how the codependence of random variables at different locations changes with the separation distance. These functions are unambiguously defined only for stationary processes. For example, the random process describing the behavior of the transistor length L is stationary only if there is non systematic spatial variation of the mean L. If the process is not stationary, the correlation function is not a reliable measure of codependence and correlation. Once the systematic wafer-level and field-level dependencies are removed, thereby making the process stationary, the true correlation is found to be negligibly small. From a statistical modeling perspective, systematic variations affect all transistors in a given circuit equally. Thus, systematic parametric variations can be represented by a deviation in the parameter mean of every transistor in the circuit.

We model the manufactured values of the parameters $p_i \in \{p_1 \ldots, p_m\}$ for transistor i as a random variable

$$p_i = \mu_{p,i} + \sigma_p(d_i) \cdot p(d_i, \theta) \qquad (1)$$

where $\mu_{p,i}$ and $\sigma_p(d_i)$ are the mean value and standard deviation of the parameter p_i, respectively, $p(d_i, \theta)$ is the stochastic process corresponding to parameter p, d_i denotes the location of transistor i on the die with respect to a point origin and
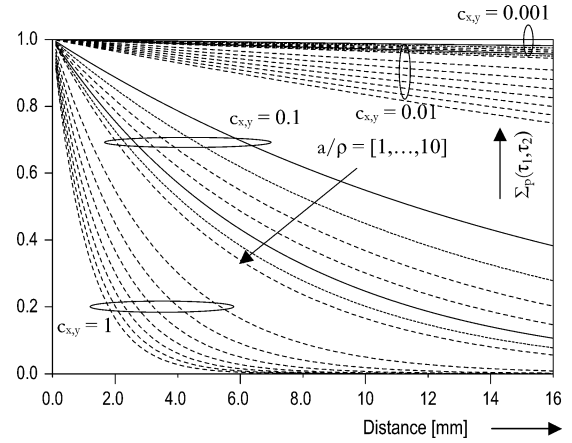

Fig. 1. Behavior of modeled covariance functions $\sum_p$ using $M = 5$ for $a/\rho = [1, \ldots, 10]$.

θ is the die on which the transistor lies. This reference point can be located, say in the lower left corner of the die, or in the center, etc. A random process can be represented as a series expansion of some uncorrelated random variables involving a complete set of deterministic functions with corresponding random coefficients. A commonly used series involves spectral expansion [23], in which the random coefficients are uncorrelated only if the random process is assumed stationary and the length of the random process is infinite or periodic. The use of the Karhunen–Loève expansion [24] has generated interest because of its biorthogonal property, that is, both the deterministic basis functions and the corresponding random coefficients are orthogonal [25], e.g., the orthogonal deterministic basis function and its magnitude are, respectively, the eigenfunction and eigenvalue of the covariance function. Assuming that p_i is a zero-mean Gaussian process and using the Karhunen–Loève expansion, p_i can be written in truncated form (for practical implementation) by a finite number of terms M as

$$p_i = \mu_{p,i} + \sigma_p(d_i) \cdot \sum_{n=1}^{M} \sqrt{\vartheta_{p,n}} \delta_{p,n}(\theta) f_{p,n}(d_i) \qquad (2)$$

where $\{\delta_n(\theta)\}$ is a vector of zero-mean uncorrelated Gaussian random variables and $f_{p,n}(d_i)$ and $\vartheta_{p,n}$ are the eigenfunctions and the eigenvalues of the covariance matrix $\sum_p(d_1, d_2)$ (Fig. 1) of $p(d_i, \theta)$, controlled through a distance based weight term, the measurement correction factor, correlation parameter ρ and process correction factors c_x and c_y.

Without loss of generality, consider for instance two transistors with given threshold voltages. In our approach, their threshold voltages are modeled as stochastic processes over the spatial domain of a die, thus making parameters of any two transistors on the die two different correlated random variables. The value of M is governed by the accuracy of the eigen-pairs in representing the covariance function rather than the number of random variables. For instance, in Fig. 1, process correction factor $c_{x,y} = 0.001$ relates to a very mature process, while $c_{x,y} = 1$ indicates that this is a process in a ramp-up phase. The correlation parameter ρ reflecting the spatial scale of clustering defined in $[-a, a]$ regulates the decaying rate of the correlation function with respect to distance (d_1, d_2) between
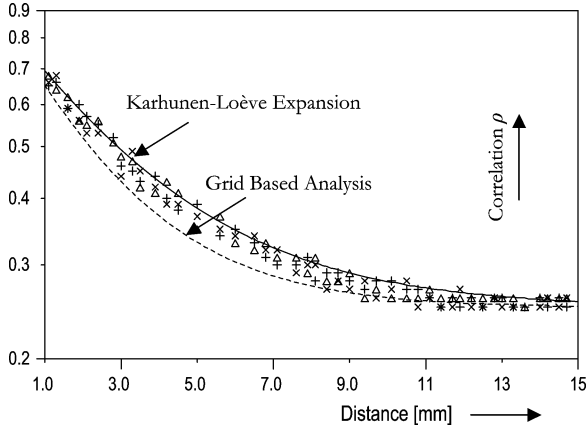
This article has been accepted for inclusion in a future issue of this journal. Content is final as presented, with the exception of pagination.

ZJAJO *et al.*: STOCHASTIC ANALYSIS OF DEEP-SUBMICROMETER CMOS PROCESS FOR RELIABLE CIRCUITS DESIGNS 3

Fig. 2. The model fitting on the available measurement data.

the two transistors located at Euclidian coordinates (x_1, y_1) and (x_2, y_2). Physically, lower a/ρ implies a highly correlated process and hence, a smaller number of random variables are needed to represent the random process and correspondingly, a smaller number of terms in the Karhunen–Loève expansion. This means that for $c_{x,y} = 0.001$ and $a/\rho = 1$, the number of transistors that need to be sampled to assess, say, a process parameter such as threshold voltage is much less than the number that would be required for $c_{x,y} = 1$ and $a/\rho = 10$ because of the high nonlinearity shown in the correlation function.

One example of spatial correlation dependence and model fitting on the available measurement data through Karhunen–Loève expansion is given in Fig. 2.

For comparison purposes, a grid-based spatial-correlation model is intuitively simple and easy to use, yet its limitations due to the inherent accuracy-versus-efficiency necessitate a more flexible approach, especially at short to midrange distances [26]. We now introduce a model $\eta_p = f(.)$, accounting for voltage and current shifts due to random manufacturing variations in transistor dimensions and process parameters defined as

$$\eta_p = f(\nu, W^*, L^*, p^*) \tag{3}$$

where ν defines a fitting parameter estimated from the extracted data, W^* and L^* represent the geometrical deformation due to manufacturing variations, and p^* models electrical parameter deviations from their corresponding nominal values, e.g., altered transconductance, threshold voltage, etc.

B. Noise Models

The most important types of electrical noise sources (thermal, shot, and flicker noise) in passive elements and integrated circuit devices have been investigated extensively, and appropriate models have been derived [9] as stationary and in [10] as nonstationary noise sources. In this paper we adapt model descriptions as defined in [10], where thermal and shot noise are expressed as delta-correlated noise processes having independent values at every time point, modeled as modulated white noise processes. These noise processes correspond to the current noise sources, which are included in the models of the integrated circuit devices.

III. STOCHASTIC MNA FOR PROCESS VARIABILITY ANALYSIS

In general, for time-domain analysis, modified nodal analysis (MNA) leads to a nonlinear ordinary differential equation (ODE) or differential algebraic equation (DAE) system, which, in most cases, is transformed into a nonlinear algebraic system by means of linear multistep integration methods [27], [28] and, at each integration step, a Newton-like method is used to solve this nonlinear algebraic system. Therefore, from a numerical point of view, the equations modeling a dynamic circuit are transformed to equivalent linear equations at each iteration of the Newton method and at each time instant of the time-domain analysis. Thus, we can say that the time-domain analysis of a nonlinear dynamic circuit consists of the successive solutions of many linear circuits approximating the original (nonlinear and dynamic) circuit at specific operating points.

Consider a linear circuit with $N+1$ nodes and B voltage-controlled branches (two-terminal resistors, independent current sources, and voltage-controlled n-ports), the latter grouped in set B. We then introduce the source current vector $\hat{i} \in R^B$ and the branch conductance matrix $G \in R^{B \times B}$. By assuming that the branches (one for each port) are ordered element by element, the matrix is block diagonal: each 1×1 block corresponds to the conductance of a one-port and in any case is nonzero, while $n \times n$ blocks correspond to the conductance matrices of voltage-controlled n-ports. More in detail, the diagonal entries of the $n \times n$ blocks can be zero and, in this case, the nonzero off-diagonal entries, on the same row or column, correspond to voltage-controlled current sources (VCCSs). Now, consider MNA and circuits embedding, besides voltage-controlled elements, independent voltage sources, the remaining types of controlled sources and sources of process variations. We split the set of branches B in two complementary subsets: B_V of voltage-controlled branches (v-branches) and B_C of current-controlled branches (c-branches). Conventional nodal analysis (NA) is extended to MNA [28] as follows: currents of c-branches are added as further unknowns and the corresponding branch equations are appended to the NA system. The $N \times B$ incidence matrix $\mathbf{A}$ can be partitioned as $\mathbf{A} = [\mathbf{A}_v \mathbf{A}_c]$, with $\mathbf{A}_v \in R^{N \times Bv}$ and $\mathbf{A}_c \in R^{N \times Bc}$. As in conventional NA, constitutive relations of v-branches are written, using the conductance submatrix $\mathbf{G}^{\cdot} \in R^{Bc \times Bv}$ in the form

$$\mathbf{i}_v = \mathbf{G}^{\cdot} \mathbf{v}_v \tag{4}$$

while the characteristics of the c-branches, including independent voltage sources and controlled sources except VCCSs, are represented by the implicit equation

$$\mathbf{B}_c \mathbf{v}_c + \mathbf{R}_c \mathbf{i}_c + \hat{\mathbf{v}}_c + \mathbf{F}_c \boldsymbol{\eta} = 0 \tag{5}$$

where $\mathbf{B}_c, \mathbf{R}_c, \mathbf{F}_c \in R^{Bc \times Bc}$, $\hat{\mathbf{v}}_c = (\mathbf{A}^T \mathbf{v}_c) \in R^{Bc}$ [27] and $\boldsymbol{\eta} \in R^{Bc}$ is a random vector accounting for device variations as defined in (3). These definitions are in agreement with those adopted in the currently used simulators and suffice for a large variety of circuits. Note that from the practical use perspective, a user may only be interested in voltage variations over a period of time or in the worst case in a period of time. This information can be obtained once the variations in any given time instance

This article has been accepted for inclusion in a future issue of this journal. Content is final as presented, with the exception of pagination.

4   IEEE TRANSACTIONS ON CIRCUITS AND SYSTEMS—I: REGULAR PAPERS

are known. By using the above notations, (4) and (5) can be written in the compact form as

$$F(\mathbf{q}', \mathbf{q}, t) + B(\mathbf{q}, t) \cdot \boldsymbol{\eta} = 0 \tag{6}$$

where $\mathbf{q} = [\mathbf{v}_c \mathbf{i}_v]^T$ is the vector of stochastic processes which represents the state variables (e.g., node voltages) of the circuit and $\boldsymbol{\eta}$ is a vector of wide-sense stationary processes. $B(\mathbf{q}, t)$ is an $N \times B_c$ matrix, the entries of which are functions of the state $\mathbf{q}$ and possibly t. Every column of $B(\mathbf{q}, t)$ corresponds to $\boldsymbol{\eta}$, and has normally either one or two nonzero entries. The rows correspond to either a node equation or a branch equation of an inductor or a voltage source. Equation (6) represents a system of nonlinear stochastic differential equations, which formulate a system of stochastic algebraic and differential equations that describe the dynamics of the nonlinear circuit that lead to the MNA equations when the random sources $\boldsymbol{\eta}$ are set to zero. Solving (6) means to determine the probability density function P of the random vector $\mathbf{q}(t)$ at each time instant t. Formally the probability density of the random variable $\mathbf{q}$ is given as

$$P(\mathbf{q}) = |\boldsymbol{\Gamma}(\mathbf{q})| N(h^{-1}(\mathbf{q})|\mathbf{m}, \boldsymbol{\Sigma}) \tag{7}$$

where $|\boldsymbol{\Gamma}(\mathbf{q})|$ is the determinant of the Jacobian matrix of the inverse transform $h^{-1}(\mathbf{q})$ with h a nonlinear function of $\boldsymbol{\eta}$. However, generally it is not possible to handle this distribution directly since it is non-Gaussian for all but linear h. Therefore it may be convenient to look for an approximation which can be found after partitioning the space of the stochastic source variables $\boldsymbol{\eta}$ in a given number of subdomains, and then solving the equation in each subdomain by means of a piecewise-linear truncated Taylor approximation. If the subdomains are small enough to consider the equation as linear in the range of variability of $\boldsymbol{\eta}$, or that the nonlinearites in the subdomains are so smooth that they might be considered as linear even for a wide range of $\boldsymbol{\eta}$, it is then possible to combine the partial results and obtain the desired approximated solution to the original problem.

Let $x_0 = x(\eta_0, t)$ be the generic point around which to linearize, and with the change of variable $\boldsymbol{\xi} = \mathbf{x} - x_0 = [(\mathbf{q} - p_0)^T, (\boldsymbol{\eta} - \eta_0)^T]^T$, the first-order Taylor piecewise-linearization of (6) in x_0 yields

$$C(x_0)\boldsymbol{\xi}' + (G(x_0) + C'(x_0))\boldsymbol{\xi} = 0 \tag{8}$$

where $G(x) = B'$, $C(x) = F'(x)$. Transient analysis requires only the solution of the deterministic version of (6), e.g., by means of a conventional circuit simulator, and of (8) with a method capable of dealing with linear stochastic differential equations with stochasticity that enters only through the initial conditions. Since (8) is a linear homogeneous equation in $\boldsymbol{\xi}$, its solution, will always be proportional to $\boldsymbol{\eta} - \eta_0$. We can rewrite (8) as

$$\boldsymbol{\xi}'(x_0) = E(x_0)\xi_0 + F(x_0)\eta_0. \tag{9}$$

Equation (9) is a system of stochastic differential equations which is linear in the narrow sense (right-hand side is linear in

ξ and the coefficient matrix for the vector of variation sources is independent of ξ) [29]. Since these stochastic processes have regular properties, they can be considered as a family of classical problems for the individual sample paths and be treated with the classical methods of the theory of linear stochastic differential equations. By expanding every element of $\xi(t)$ with

$$\boldsymbol{\xi}_i(t) = \Gamma(t)(\boldsymbol{\eta} - \eta_0) = \sum_{j=1}^m \alpha_{ij}(t) \cdot \eta_j \tag{10}$$

for m elements of a vector $\boldsymbol{\eta}$. As long as $\alpha_j(t)$ is obtained, the expression for $\boldsymbol{\xi}(t)$ is known, so that the covariance matrix of the solution can be written as

$$\boldsymbol{\Sigma}_{\xi\xi} = \boldsymbol{\Gamma}\boldsymbol{\Sigma}_{\eta\eta}\boldsymbol{\Gamma}^T. \tag{11}$$

Defining $\alpha_j(t) = (\alpha_{1j}, \alpha_{2j}, \ldots, \alpha_{nj})^T$, $F_j(t) = (F_{1j}, F_{2j}, \ldots, F_{nj})^T$, the requirement for $\alpha(t)$ is

$$\alpha_j'(t) = E(t)\alpha_j + F(t) \tag{12}$$

Equation (12) is an ordinary differential equation, which can be solved by a fast numerical method.

IV. STOCHASTIC MNA FOR NOISE ANALYSIS

The inherent nature of white noise process $\boldsymbol{\chi}$ differ fundamentally from a wide-sense stationary stochastic process such as static manufacturing variability and cannot be treated as an ordinary differential equation using similar differential calculus as in Section III. The MNA formulation of the stochastic process that describes random influences which fluctuate rapidly and irregularly (i.e., white noise $\boldsymbol{\chi}$) can be written as

$$F(\mathbf{r}', \mathbf{r}, t) + B(\mathbf{r}, t) \cdot \boldsymbol{\chi} = 0 \tag{13}$$

where $\mathbf{r}$ is the vector of stochastic processes which represents the state variables (e.g., node voltages) of the circuit, $\boldsymbol{\chi}$ is a vector of white Gaussian processes, and $B(\mathbf{r}, t)$ is a state- and time-dependent modulation of the vector of noise sources. Since the magnitude of the noise content in a signal is much smaller in comparison to the magnitude of the signal itself in any functional circuit, a system of nonlinear stochastic differential equations described in (13) can be piecewise-linearized under similar assumptions as noted in the previous section. Now, including the noise content description, (9) can be expressed in general form as

$$\lambda'(t) = E(t)\lambda + F(t)\chi \tag{14}$$

where $\boldsymbol{\lambda} = [(\mathbf{r} - r_0)^r \cdot (\boldsymbol{\chi} - \chi_0)^T]^T$. We will interpret (14) as an Ito system of stochastic differential equations. Now rewriting (14) in the more natural differential form

$$d\lambda(t) = E(t)\lambda dt + F(t)dw \tag{15}$$

where we substituted $dw(t) = \chi(t)dt$ with a vector of Wiener process w. If the functions $E(t)$ and $F(t)$ are measurable and bounded on the time interval of interest, there exists a unique solution for every initial value $\lambda(t_0)$ [29].

This article has been accepted for inclusion in a future issue of this journal. Content is final as presented, with the exception of pagination.

ZJAJO *et al.*: STOCHASTIC ANALYSIS OF DEEP-SUBMICROMETER CMOS PROCESS FOR RELIABLE CIRCUITS DESIGNS

5

If λ is a Gaussian stochastic process, then it is completely characterized by its mean and correlation function. From Ito's theorem on stochastic differentials

$$\frac{d(\lambda(t)\lambda^T(t))}{dt} = \lambda(t) \cdot \frac{d(\lambda^T(t))}{dt} + \frac{d(\lambda(t))}{dt} \cdot \lambda^T(t) + F(t) \cdot F^T(t)dt \qquad (16)$$

and expanding (16) with (15), noting that λ and dw are uncorrelated, variance-covariance matrix $\mathbf{K}(t)$ of $\boldsymbol{\lambda}(t)$ with the initial value $\mathbf{K}(0) = E[\lambda \lambda^T]$ can be expressed in differential Lyapunov matrix equation form as [29]

$$\frac{d\mathbf{K}(t)}{dt} = \mathbf{E}(t)\mathbf{K}(t) + \mathbf{K}(t)\mathbf{E}^T(t) + \mathbf{F}(t)\mathbf{F}^T(t). \qquad (17)$$

Note that the mean of the noise variables is always zero for most integrated circuits. In view of the symmetry of $\mathbf{K}(t)$, (17) represents a system of linear ordinary differential equations with time-varying coefficients. To obtain a numerical solution, (17) has to be discretized in time using a suitable scheme, such as any linear multistep method, or a Runge–Kutta method. For circuit simulation, implicit linear multistep methods, and especially the trapezoidal method and the backward differentiation formula were found to be most suitable [30]. If backward Euler is applied to (17), the differential Lyapunov matrix equation can be written in a special form referred to as the continuous-time algebraic Lyapunov matrix equation

$$\mathbf{P}_r\mathbf{K}(t_r) + \mathbf{K}(t_r)\mathbf{P}_r^T + \mathbf{Q}_r = 0. \qquad (18)$$

$\mathbf{K}(t)$ at time point t_r is calculated by solving the system of linear equations in (18). Such continuous time Lyapunov equations have a unique solution $\mathbf{K}(t)$, which is symmetric and positive semidefinite.

Several iterative techniques have been proposed for the solution of the algebraic Lyapunov matrix equation (18) arising in some specific problems where the matrix $\mathbf{P}_r$ is large and sparse [31]–[34], such as the Bartels–Stewart method [35], and Hammarling's method [29], which remains the one and only reference for directly computing the Cholesky factor of the solution $\mathbf{K}(t_r)$ of (18) for small to medium systems. For the backward stability analysis of the Bartels–Stewart algorithm, see [36]. Extensions of these methods to generalized Lyapunov equations are described in [37]. In the Bartels–Stewart algorithm, first $\mathbf{P}_r$ is reduced to upper Hessenberg form by means of Householder transformations, and then the QR-algorihm is applied to the Hessenberg form to calculate the real Schur decomposition [38] to transform (18) to a triangular system which can be solved efficiently by forward or backward substitutions of the matrix $\mathbf{P}_r$

$$\mathbf{S} = \mathbf{U}^T\mathbf{P}_r\mathbf{U} \qquad (19)$$

where the real Schur form $\mathbf{S}$ is upper quasi-triangular and $\mathbf{U}$ is orthonormal. Our formulation for the real case utilizes a similar scheme. The transformation matrices are accumulated at each step to form $\mathbf{U}$[35]. If we now set

$$\tilde{\mathbf{K}} = \mathbf{U}^T\mathbf{K}(t_r)\mathbf{U}$$
$$\tilde{\mathbf{Q}} = \mathbf{U}^T\mathbf{Q}_r\mathbf{U} \qquad (20)$$

then (18) becomes

$$\mathbf{S}\tilde{\mathbf{K}} + \tilde{\mathbf{K}}\mathbf{S}^T = -\tilde{\mathbf{Q}}. \qquad (21)$$

To find a unique solution, we partition (21) as

$$\mathbf{S} = \begin{bmatrix} \mathbf{S}_1 & \mathbf{s} \\ \mathbf{0} & v_n \end{bmatrix} \tilde{\mathbf{K}} = \begin{bmatrix} \mathbf{K}_1 & \mathbf{k} \\ \mathbf{k}^T & k_{nn} \end{bmatrix}$$
$$\tilde{\mathbf{Q}} = \begin{bmatrix} \mathbf{Q}_1 & \mathbf{q} \\ \mathbf{q}^T & q_{nn} \end{bmatrix}$$

where $\mathbf{S}_1, \mathbf{K}_1, \mathbf{Q}_1 \in C^{(n-1)\times(n-1)}$; $s, k, q \in C^{(n-1)}$. The system in (21) then gives three equations

$$(v_n + \bar{v}_n)k_{nn} + q_{nn} = 0 \qquad (22)$$
$$(\mathbf{S}_1 + \bar{v}_n\mathbf{I})\mathbf{k} + \mathbf{q} + k_{nn}\mathbf{s} = \mathbf{0} \qquad (23)$$
$$\mathbf{S}_1\mathbf{K}_1 + \mathbf{K}_1\mathbf{S}_1^T + \mathbf{Q}_1 + \mathbf{s}\mathbf{k}^T + \mathbf{k}\mathbf{s}^T = \mathbf{0}. \qquad (24)$$

k_{nn} can be obtained from (22) and set in (23) to solve for $\mathbf{K}$. Once $\mathbf{K}$ is known, (24) becomes a Lyapunov equation which has the same structure as (21) but of order $(n-1)$, as

$$\mathbf{S}_1\mathbf{K}_1 + \mathbf{K}_1\mathbf{S}_1^T = -\mathbf{Q}_1 - \mathbf{s}\mathbf{k}^T - \mathbf{k}\mathbf{s}^T. \qquad (25)$$

We can apply the same process to (25) until $\mathbf{S}_1$ is of the order -1. Note under the condition that $i = 1, \dots, n$ at the kth step $(k = 1, 2, \dots, n)$ of this process, we can obtain a unique solution vector of length $(n+1-k)$ and a reduced triangular matrix equation of order $(n-k)$. Since $\mathbf{U}$ is orthonormal, once (21) is solved for $\tilde{\mathbf{K}}$, then $\mathbf{K}(t_r)$ can be computed using

$$\mathbf{K}(t_r) = \mathbf{U}\tilde{\mathbf{K}}\mathbf{U}^T. \qquad (26)$$

Large dense Lyapunov equations can be solved by sign function based techniques [38]. Krylov subspace methods, which are related to matrix polynomials have been proposed [40] as well. Relatively large sparse Lyapunov equations can be solved by iterative approaches, e.g., [41]. In this paper, we apply a low rank version of the iterative method [42], which is related to rational matrix functions. The postulated iteration for the Lyapunov (18) is given by $\mathbf{K}(0) = 0$ and

$$(P_r + \gamma_i I_n)K_{i-1/2} = -Q_r - K_{i-1}(P_r^T - \gamma_i I_n)$$
$$(P_r + \bar{\gamma}_i I_n)K_i^T = -Q_r - K_{i-1/2}^T(P_r^T - \bar{\gamma}_i I_n) \qquad (27)$$

for $i = 1, 2, \dots$ This method generates a sequence of matrices $\mathbf{K}_i$ which often converges very fast towards the solution, provided that the iteration shift parameters γ_i are chosen (sub)optimally. For a more efficient implementation of the method, we replace iterates by their Cholesky factors, i.e., $K_i = L_iL_i^H$ and reformulate in terms of the factors L_i. The low rank Cholesky factors L_i are not uniquely determined. Different ways to generate them exist [42]. Note that the number of iteration steps

This article has been accepted for inclusion in a future issue of this journal. Content is final as presented, with the exception of pagination.

6   IEEE TRANSACTIONS ON CIRCUITS AND SYSTEMS—I: REGULAR PAPERS

$i_{\max}$ needs not be fixed *a priori*. However, if the Lyapunov equation should be solved as accurate as possible, correct results are usually achieved for low values of stopping criteria which are slightly larger than the machine precision.

V. SIMULATION ACCURACY

In general, there are three sources which can cause loss of simulation accuracy. The first source is due to the structural approximation of the original circuit block by the primitive, although it is more general than the conventional inverter type primitive and therefore introduces less error. This mapping problem is universal in large-scale digital simulation and cannot be avoided. The second source of error is due to the use of second-order polynomial models for the I–V characteristics of MOS transistors. The threshold-voltage-based models, such as BSIM and MOS 9, make use of approximate expressions of the drain-source channel current I_{DS} in the weak inversion region and in the strong-inversion region. These approximate equations are tied together using a mathematical smoothing function, resulting in neither a physical nor an accurate description of I_{DS} in the moderate inversion region. The major advantages of surface potential [43] over threshold voltage based models is that surface potential models do not rely on the regional approach and I–V and C–V characteristics in all operation regions are expressed/evaluated using a set of unified formulas. Numerical progress has also removed a major concern in surface potential modeling: the solution of the surface potential either in a closed form (with limited accuracy) exists or with use of the second-order Newton iterative method to improve the computational efficiency in MOS model 11 [44]. The third source of error is due to the piecewise-linear approximation. Conventionally, the piecewise-linear approximation is done implicitly in the timing analysis process. Since the information on the whole waveform is not available until the timing analysis is completed, the piecewise-linear waveforms generated as such in a noise environment can not always approximate nonfully-switching waveforms and glitches and thus can cause significant errors. The piecewise-linear approximation greatly improves calculation speed and allows direct approach. The precision of our models is in line with the piecewise-linear models used in industry practice. If better precision is required, more advanced optimum filter models (e.g., extended or unscented Kalman–Bucy, etc.) can be employed, however, at the cost of a decreased calculation speed.

The voltage nodes and current branches in the integrated circuits and systems, which are time varying, can be formulated as stochastic state space models, and the time evolution of the system can be estimated using optimal filters. We model the state transitions as a Markovian switching system, which is perturbed by a certain process noise. This noise is used for modeling the uncertainties in the system dynamics and in most cases the system is not truly stochastic, but the stochasticity is only used for representing the model uncertainties. The model is defined as

$$\begin{aligned}
\mathbf{x}_k &= \mathbf{f}(\mathbf{x}_{k-1}, k-1) + \mathbf{d}_{k-1} \\
\mathbf{y}_k &= \mathbf{h}(\mathbf{x}_k, k) + \mathbf{l}_k
\end{aligned} \tag{28}$$

where $\mathbf{x}_k \in C^n$ is the state, $\mathbf{y}_k \in C^m$ is the measurement, $\mathbf{d}_{k-1} \sim N(\mathbf{0}, \mathbf{D}_{k-1})$ is the Gaussian process noise, $\mathbf{l}_k \sim N(\mathbf{0}, \mathbf{L}_k)$ is the Gaussian measurement noise, $\mathbf{f}(.)$ is the dynamic model function and $\mathbf{h}(.)$ is the measurement model function. The idea of constructing mathematically optimal recursive estimators was first presented for linear systems due to their mathematical simplicity and the most natural optimality criterion from both the mathematical and modeling points of view is least squares optimality. For linear systems the optimal solution coincides with the least squares solution, that is, the optimal least squares solution is exactly the calculated mean. However, the problem of (least squares) optimal filtering can only be applied to stationary signals and construction of such a filter is often mathematically demanding. As a result an efficient solution can only be found for simple low dimensional problems. On the other hand, the recursive solution to the optimal linear filtering problem containing a least square filter as its limiting special case offers a much simpler mathematical approach. Because computing the full joint distribution of the states at all time steps is computationally very inefficient and unnecessary in real-time applications, our objective is to compute distributions

$$P(\mathbf{x}_k|\mathbf{y}_{1:k}) \approx N(\mathbf{x}_k|\mathbf{m}_k, \mathbf{\Sigma}_k) \tag{29}$$

recursively in a sense that the previous computations do not need to be redone at each step and the amount of computations is, in principle, constant per time step. Defining the prediction step with the Chapman–Kolmogorov equation
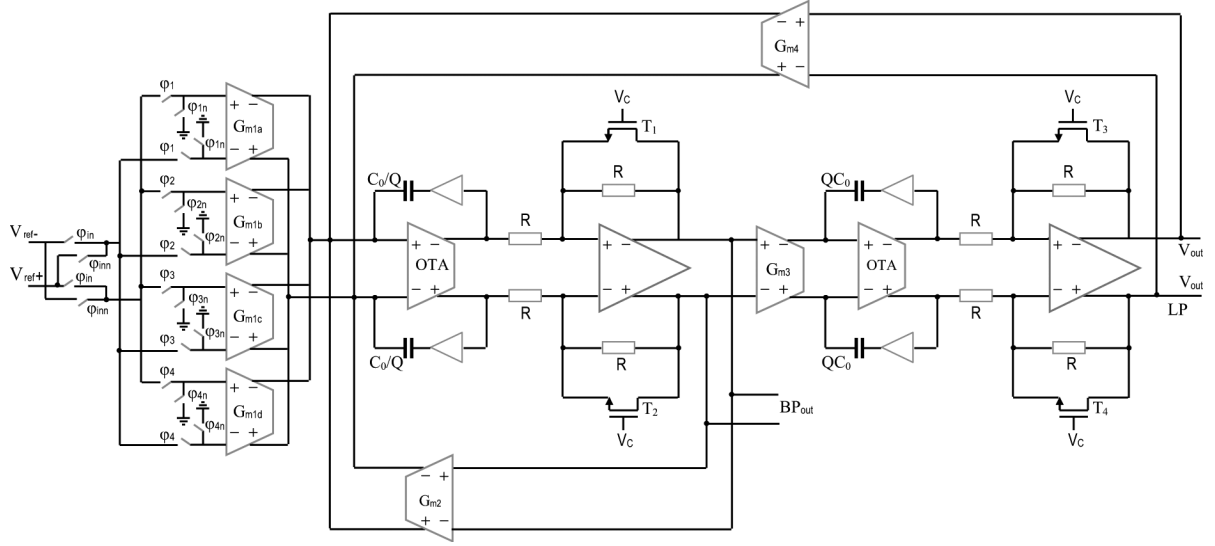
$$\begin{aligned}
\mathbf{m}_k^- &= \mathbf{f}(\mathbf{m}_{k-1}, k-1) \\
\mathbf{\Sigma}_k^- &= \mathbf{\Gamma}_x(\mathbf{m}_{k-1}, k-1)\mathbf{\Sigma}_{k-1}\mathbf{\Gamma}_x^T \\
&\quad \times (\mathbf{m}_{k-1}, k-1) + \mathbf{D}_{k+1}
\end{aligned} \tag{30}$$

the update step can be found with

$$\begin{aligned}
\mathbf{v}_k &= \mathbf{y}_k - \mathbf{h}(\mathbf{m}_k^-, k) \\
\mathbf{Z}_k &= \mathbf{H}_x(\mathbf{m}_k^-, k)\mathbf{\Sigma}_k^-\mathbf{H}_x^T(\mathbf{m}_k^-, k) + \mathbf{L}_k \\
\mathbf{B}_k &= \mathbf{\Sigma}_k^-\mathbf{H}_x^T(\mathbf{m}_k^-, k)\mathbf{Z}_k^{-1} \\
\mathbf{m}_k &= \mathbf{m}_k^- + \mathbf{B}_k\mathbf{v}_k \\
\mathbf{\Sigma}_k &= \mathbf{\Sigma}_k^- - \mathbf{B}_k\mathbf{Z}_k\mathbf{B}_k^T
\end{aligned} \tag{31}$$

where $\mathbf{v}_k$ is the residual of the prediction, $\mathbf{Z}_k$ is the measurement prediction covariance in the time step k, and $\mathbf{B}_k$ designates the prediction correction in time step k. The matrices $\mathbf{\Gamma}_x(\mathbf{m}, k-1)$ and $\mathbf{H}_x(\mathbf{m}, k)$ are the Jacobian matrices of f and h, respectively. Note that in this case the predicted and estimated state covariances on different time steps do not depend on any measurements. Similarly, optimal smoothing methods have evolved at the same time as filtering methods, and as in the filtering case the optimal smoothing equations can be solved in closed form only in a few special cases The linear Gaussian case is such a special case, and it leads to the Rauch–Tung–Striebel smoother. Following the notation given in (31), the smoothing solution for the model (28) is computed as

$$\begin{aligned}
\mathbf{m}_{k+1}^- &= \mathbf{f}(\mathbf{m}_k, k) \\
\mathbf{\Sigma}_{k+1}^- &= \mathbf{\Gamma}_x(\mathbf{m}_k, k)\mathbf{\Sigma}_k\mathbf{\Gamma}_x^T(\mathbf{m}_k, k) + \mathbf{D}_k
\end{aligned}$$

This article has been accepted for inclusion in a future issue of this journal. Content is final as presented, with the exception of pagination.

ZJAJO *et al.*: STOCHASTIC ANALYSIS OF DEEP-SUBMICROMETER CMOS PROCESS FOR RELIABLE CIRCUITS DESIGNS 7

Fig. 3. $G_m - C - OTA$ biquad filter [31].

$$\mathbf{B}_k = \mathbf{\Sigma}_k \mathbf{\Gamma}_x^T(\mathbf{m}_k, k)[\mathbf{\Sigma}_{k+1}^-]^{-1}$$
$$\mathbf{m}_k^s = \mathbf{m}_k + \mathbf{B}_k[\mathbf{m}_{k+1}^s - \mathbf{m}_{k+1}^-]$$
$$\mathbf{\Sigma}_k^s = \mathbf{\Sigma}_k + \mathbf{B}_k[\mathbf{\Sigma}_{k+1}^s - \mathbf{\Sigma}_{k+1}^-]\mathbf{B}_k^T \qquad (32)$$

VI. Experimental Results

All proposed methods and all sparse techniques have been implemented in Matlab. All the experimental results are carried out on a single processor Linux system with Intel Core 2 Duo CPUs with 2.66 Ghz and 3 GB of memory. In order to be able to perform a statistical simulation, the proposed method requires, in addition to a netlist description of the circuit written in the language of currently used simulators such as Spice or Spectre, some supplementary information on the circuit geometries and on extra stochastic parameters describing the random sources. The geometric information may be readily obtained by a layout view of the circuit available in standard CAD tools, or may be entered by the user should the layout not be available at the current design stage. The stochastic parameters are related to a specific technology, and may be extracted as pointed out in Section II. When all the necessary parameters for the statistical simulation are available, these parameters, together with the output of the conventional simulator, enable, with the proposed method, to solve either the stochastic linear differential equations describing the circuit influenced by the process variations (11) or the set of linear time-varying (18) including the noise content description to get the steady state value of the time-varying covariance matrix. This gives the variance at the output node and its cross correlation with other nodes in the circuit. The covariance matrix is periodic with the same period as either the input signal (e.g., translinear circuits) or the clock (in circuits such as switched capacitor circuits).

The effectiveness of the proposed approaches was evaluated on several circuits exhibiting different distinctive features in a variety of applications. As one of the representative examples of the results that can be obtained, we show firstly an application of statistical simulation to the characterization of the continuous-time bandpass $G_m - C - OTA$ biquad filter [45]
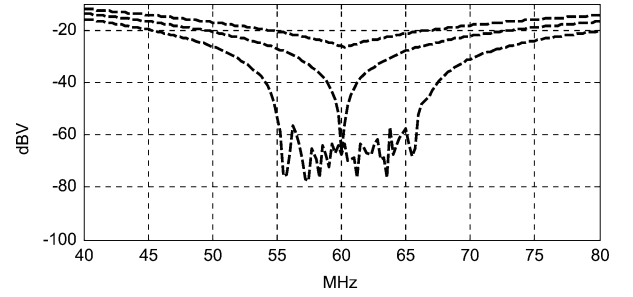
Fig. 4. $G_m - C - OTA$ biquad filter frequency response. Middle line designates the nominal behavior.
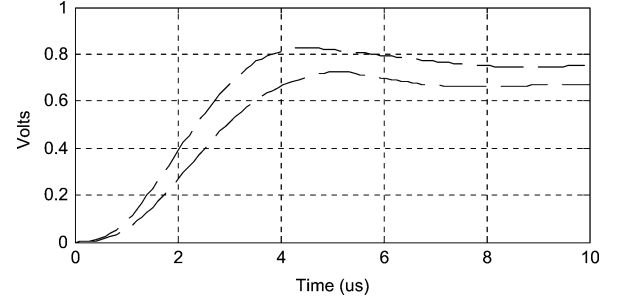
Fig. 5. Transient response of $G_m - C - OTA$ biquad filter.

(Fig. 3) with the frequency response illustrated in Fig. 4. The implemented double feedback structure yields an overall improvement on the filter linearity performance. With the opposite phase of the distortion amount introduced by the transconductors in the feedback path, the smaller loop (with G_{m2}) partially attenuates the nonlinearity deriving from transconductor G_{m3}, whereas the larger loop (with G_{m4}) attenuates the nonlinearity deriving from the input G_{m1}. The transconductor G_{m2} introduces some partial positive feedback (acts as a negative resistor) so that the quality factor can be made as high as desired, only limited by parasitics and stability issues. The filter cut-off frequency is controlled through G_{m3} and G_{m4}, the Q-factor is controlled through a G_{m2}, and the gain can be set with G_{m1}. The calculated transient response of the filter is illustrated in Fig. 5. In comparison with Monte Carlo analysis (it can be shown that

This article has been accepted for inclusion in a future issue of this journal. Content is final as presented, with the exception of pagination.

8

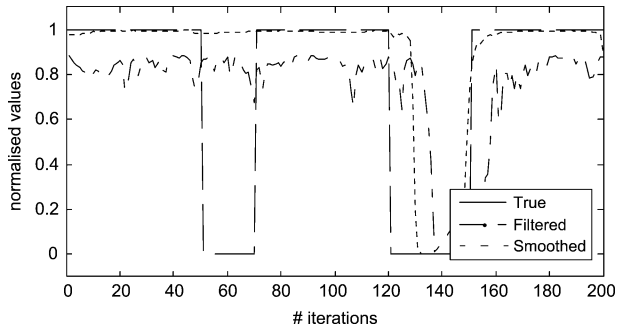IEEE TRANSACTIONS ON CIRCUITS AND SYSTEMS—I: REGULAR PAPERS

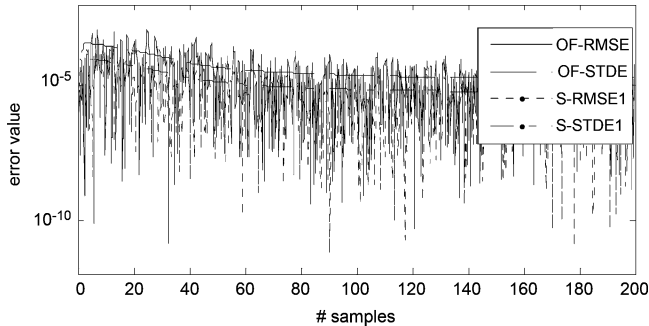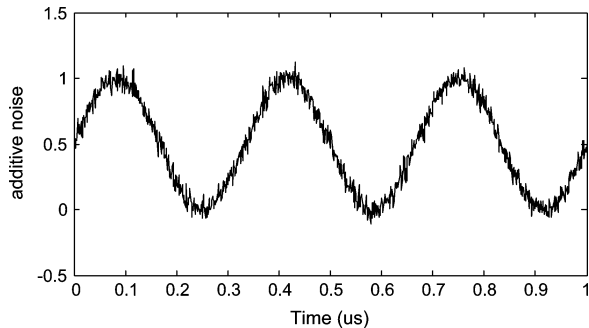Fig. 6. Probability of the proposed model.

Fig. 7. RMSE of estimating parameter x with optimal filter and smoothing algorithm for biquad filter.

Fig. 8. Time series with additive Gaussian noise.

Fig. 9. Estimation of noise variance.

Fig. 10. Stopping criterion: maximal number of iteration steps.

1500 iterations are necessary to accurately represent the performance function) the difference is less then 1% and 3% for mean and variance, respectively, while significant gain on the *cpu*-time is achieved (12.2 s versus 845.3 s). Similarly, in comparison with the measured transient response (measured across 25 prototype samples), the calculated variance is within 5%. In Fig. 6 we have plotted the filtered and smoothed estimates of the probabilities of the model in each time step. It can be seen that it takes some time for the filter to respond to model transitions. As expected, smoothing reduces this lag as well as giving substantially better overall performance. The quality criterion adopted for estimating parameter x with an optimal filter and smoothing algorithm is the root-mean-squared error (RMSE) criterion, mainly because it represents the energy in the error signal, is easy to differentiate and provides the possibilities to assign weights (Fig. 7). For noise simulations we have included only the shot and thermal noise sources as including the flicker noise sources increases the simulation time due to the large time constants introduced by the networks for flicker noise source synthesis.

We assumed that the time series $\mathbf{r}$ are composed of a smoothly varying function, plus additive Gaussian white noise $\boldsymbol{\chi}$ (Fig. 8),
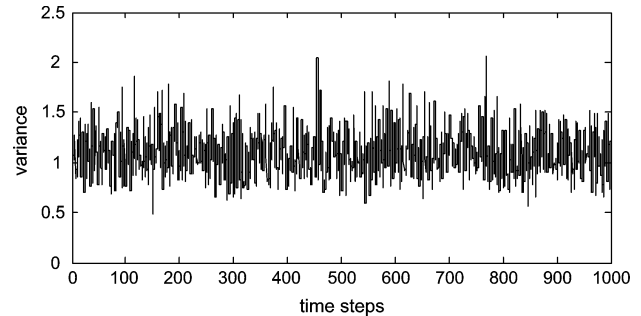
and that at any point $\mathbf{r}$ can be represented by a low order polynomial (a truncated local Taylor series approximation). This is achieved by trimming off the tails of the distributions and then using percentiles to reverse the desired variance. However, this process increases simulation time and introduces bias in the results. Inadvertently, this bias is a function of the series length and as such predictable, so the last steps in noise estimation are to filter out that predicted bias from the estimated variance. The results of the estimation of the noise variance are illustrated in Fig. 9. In comparison with 1500 Monte Carlo iterations, the difference is less then 1% and 4% for mean and variance, respectively, with considerable *cpu*-time reduction (1241.7 s versus 18.6 s). Similarly, the noise figure measured across 25 samples is within 5% of the simulated noise figure obtained as average noise power calculated over the periodic noise variance waveform.

The Bartels–Stewart algorithm and Hammarling's method carried out explicitly (as done in Matlab) can exploit the advantages provided by modern high performance computer hardware, which contains several levels of cache memories. For the recursive algorithms presented here it is observed that a faster lowest level kernel solver (with suitable block size) leads to an efficient solver of triangular matrix equations. For models with large dimension N_c and N_v, usually the matrix $\mathbf{P}_r$ has a banded or a sparse structure and applying the Bartels–Stewart type algorithm becomes impractical due to the Schur decompositions (or Hessenberg–Schur), which cost expensive $O(N^3)$ flops. In comparison with the standard Matlab function *lyap.m*, the *cpu*-time shows that computing the Cholesky factor directly is faster by approximately N flops. Similarly, when the original matrix equation is real, using real arithmetic is faster than using complex arithmetic. Hence we resort to iterative projection methods when N_c and N_v are large, and the Bartels–Stewart type algorithms including the ones presented in this paper become suitable for the reduced

This article has been accepted for inclusion in a future issue of this journal. Content is final as presented, with the exception of pagination.

ZJAJO *et al.*: STOCHASTIC ANALYSIS OF DEEP-SUBMICROMETER CMOS PROCESS FOR RELIABLE CIRCUITS DESIGNS 9
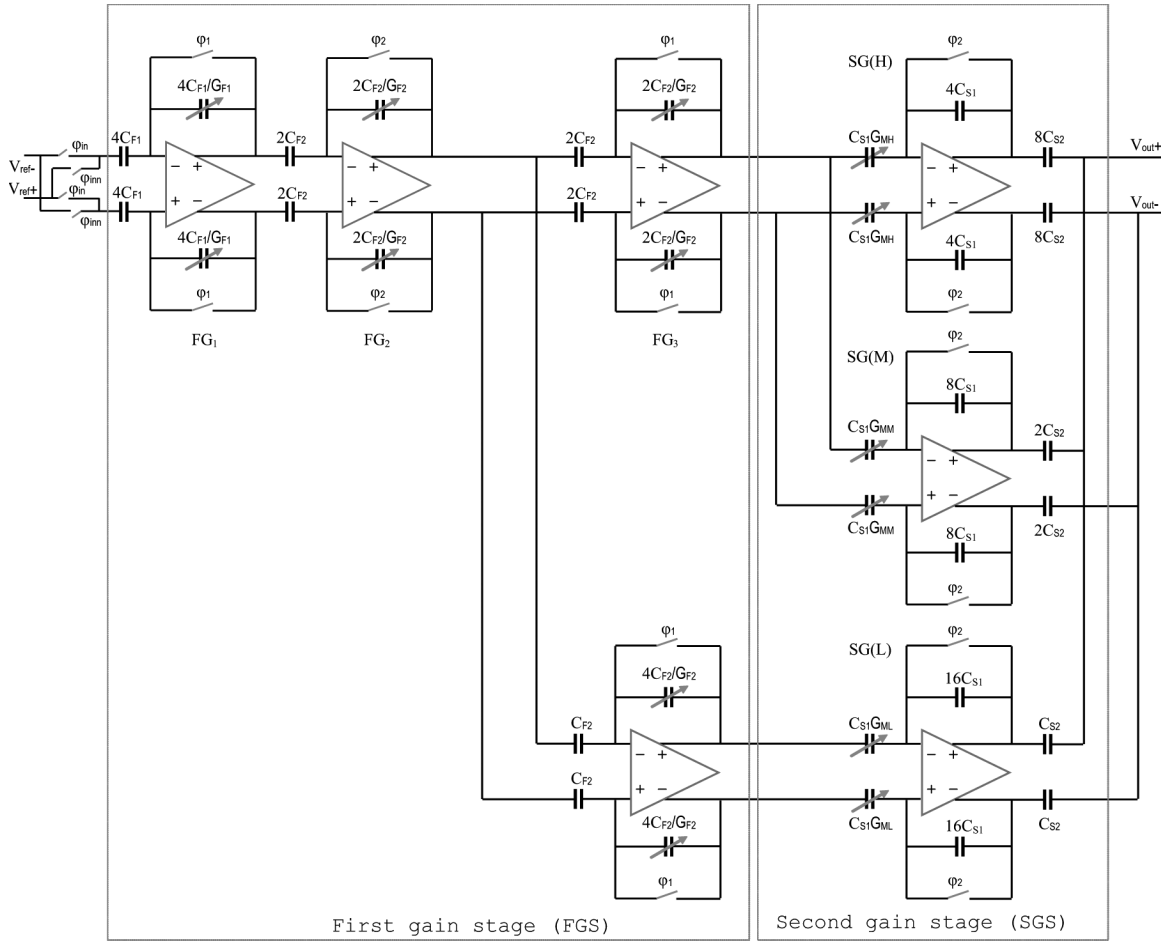
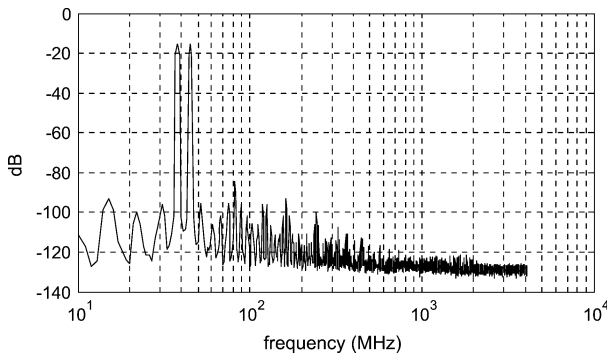

Fig. 11. Switched capacitor variable gain amplifier.

Fig. 12. SC variable gain amplifier frequency response.

small to medium matrix equations. The approximate solution of the Lyapunov equation is given by the low rank Cholesky factor L, for which $LL^H \sim K$. L has typically fewer columns than rows. In general, L can be a complex matrix, but the product LL^H is real. More precisely, the complex low rank Cholesky factor delivered by the iteration is transformed into a real low rank Cholesky factor of the same size, such that both low rank Cholesky factor products are identical. However, doing this requires additional computation. The iteration is stopped after *a priori* defined iteration steps (Fig. 10) as in [46].

The second evaluated circuit is switched capacitor (SC) variable gain amplifier illustrated in Fig. 11. The frequency response of the circuit is shown in Fig. 12. The circuit employs

two pipelined stages. The first stage is designed to have a coarse gain tuning control while the second stage provides the fine gain tuning. The circuit includes seven fully differential amplifiers and high-resolution capacitive banks for accurate segments definition of a discrete-time periodic analog signal. The first gain stage (FGS) is a cascade of three amplifiers of FG_1, FG_2, and FG_3 while the second gain stage (SGS) is designed with a parallel connection of three weighted gain amplifiers of SG(H), SG(M), and SG(L). Each pipelined cascaded SC amplifier operates with two clocks, φ_1 and φ_2, which are nonoverlapping. In the φ_1 phase, the reference signal is sampled at the input capacitors of the first stage to be transferred, and in the next phase, on the feedback capacitor. Simultaneously, the output signal of the first stage is sampled by the input capacitor of the next stage. Each stage of Fig. 11 operates in the same manner. The gain in the first stage is set by the feedback capacitance. For example, in the first pipelined amplifier stage FG_1, the input capacitance is chosen as $4C_{F1}$, and the feedback capacitance is then given by $4C_{F1}/G_{F1}$, where $G_{F1} = 1$, 2, or 4. In the second stage, the gain is set by the input capacitance. The high resolution of the gain is achieved by the parallel connection of three SC amplifiers. To illustrate that, consider, the SG(H) stage, where the input capacitance is chosen as $C_{S1} \times G_{MH}$ with $G_{MH} = 2, 3, \ldots, 7$, so that the gain is set to $CS1 \times G_{MH}/4C_{S1} = G_{MH}/4$. The calculated transient response of the circuit is illustrated in Fig. 13. In comparison
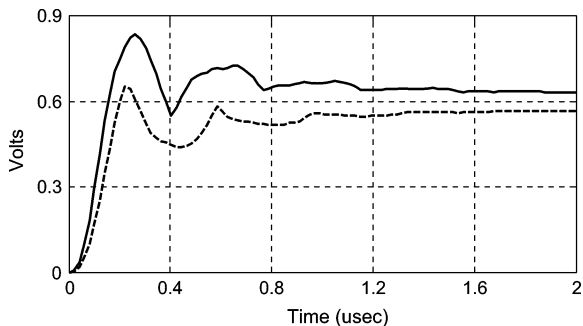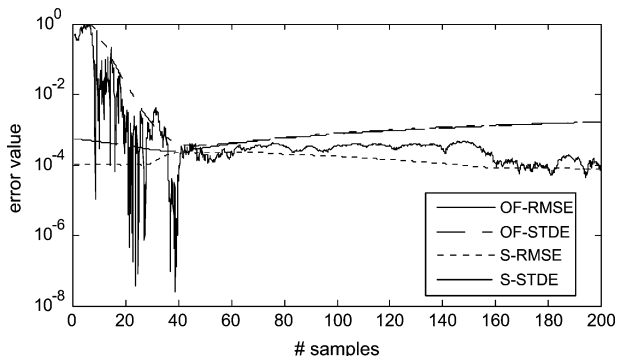
Fig. 13.   Transient response of SC variable gain amplifier.

Fig. 14.   RMSE of estimating parameter x with optimal filter and smoothing algorithm for variable gain amplifier.
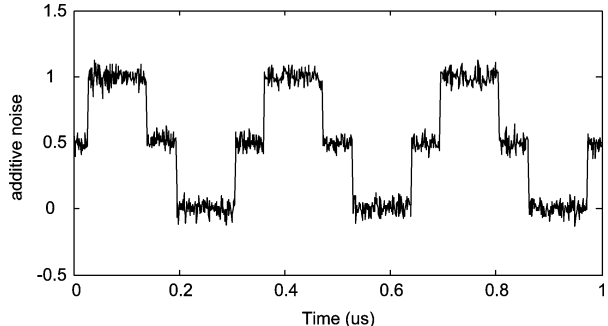

Fig. 15.   Noise estimation for functions with multiple discontinuities.

Fig. 16.   Estimation of noise variance.

Fig. 17.   Maximal number of iteration steps.

with 1500 Monte Carlo iterations, the difference is less then 1% and 5% for mean and variance, respectively, with considerable *cpu*-time reduction (1653.2 s versus 23.8 s). Similarly, the measured transient response (across 25 samples) is within 5% of the calculated variance. Fig. 14 illustrates the RMSE of estimating parameter x with optimal filter and smoothing algorithm.

When the gain is changed in discrete steps, there may be a transient in the output signal. There are two different causes of transients when the gain of a variable gain amplifier is changed. The first is the amplification of a *dc* offset with a programmable gain, which produces a step in the output signal even when the amplifier has no internal *dc* offsets or device mismatches. Secondly, when the gain of a programmable gain amplifier is changed in a device, in which a *dc* current flows, the *dc* offset at the output may be changed due to device mismatches, even when there is no *dc* offset at the input of the amplifier. In the first case, the cause of a transient is in the input signal, which contains a *dc* offset. In the latter case, the output *dc* offset of the programmable gain amplifier depends on the gain setting because of changes in the biasing, i.e., the topology of the VGA and mismatches cause the transients. The step caused by a change in the programmable gain may be a combination of both effects, although if properly deployed, the following high-frequency low-pass filtering stage will filter out this step if a sufficiently small time constant is deployed.

Noise estimation is robust to a few arbitrary spikes or discontinuities in the function or its derivatives (Fig. 15). Since any voltage at any time in a SC circuit can be expressed as a linear combination of capacitor voltages and independent voltage sources, we are interested in the time evolution of the set of all capacitor voltages.
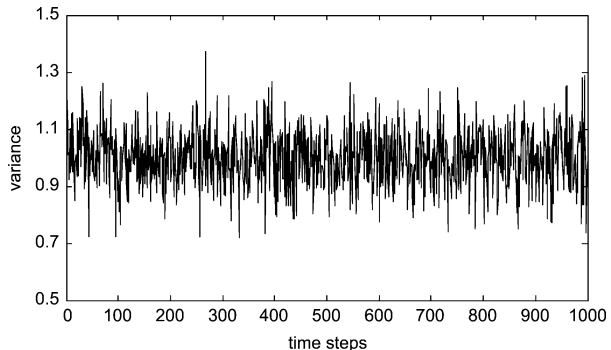
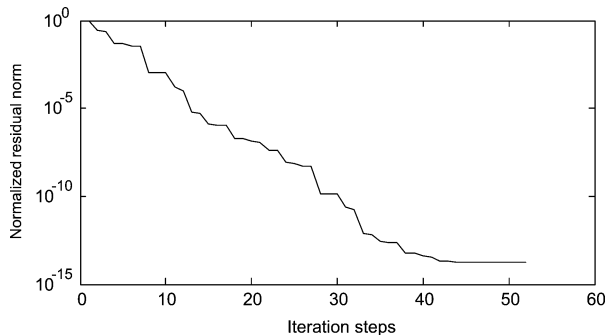Note that in our case where the independent voltage sources are white noise, the modeling has to be such that any physical voltage is a linear combination of capacitor voltages only; the mathematical fiction of white noise inhibits it from being observed as a nonfiltered process. To simplify computations the capacitor voltage variance, matrices at the end of the time slots are computed as for stationary processes, i.e., for each time slot we consider the corresponding continuous time circuit driven by white noise and determine the variance matrix of the stationary capacitor voltage processes. The results of the estimation of the noise variance are illustrated in Fig. 16. In comparison with 1500 Monte Carlo iterations, the difference is less then 1% and 6% for mean and variance, respectively, with considerable *cpu*-time reduction (2134.3 s versus 26.8 s). The noise figure measured across 25 samples is within 7% of the simulated noise figure obtained similarly as in the previous example. Fig. 17 illustrates the maximal number of iteration steps of a low rank version of the iterative method.

VII. CONCLUSION

Statistical simulation is one of the foremost steps in the evaluation of successful high-performance IC designs due

This article has been accepted for inclusion in a future issue of this journal. Content is final as presented, with the exception of pagination.

ZJAJO *et al.*: STOCHASTIC ANALYSIS OF DEEP-SUBMICROMETER CMOS PROCESS FOR RELIABLE CIRCUITS DESIGNS

11

to process variations and circuit noise which strongly affect devices behavior in today's deep submicrometer technologies. In this paper, rather than estimating statistical behavior of the circuit by a population of realizations, we describe integrated circuits as a set of stochastic differential equations and introduce Gaussian closure approximations to obtain a closed form of moment equations. The static manufacturing variability and dynamic statistical fluctuation are treated separately. Process variations are modeled as a wide-sense stationary process and the solution of MNA for such a process is found. On the other hand, noise is a nonstationary process and can not be treated directly as process variation. For this purpose Ito stochastic differentials are introduced and effective solution for Lyapunov equations found. The effectiveness of the proposed approaches was evaluated on several circuits with the continuous-time bandpass biquad filter and the discrete-time variable gain amplifier as representative examples. As the results indicate, the suggested numerical methods provide accurate and efficient solutions of stochastic differentials for both process variation and noise analysis of various scales of integrated circuits.

REFERENCES

[1] K. Bowman and J. Meindl, "Impact of within-die parameter fluctuations on the future maximum clock frequency distribution," in *Proc. IEEE Custom Integr. Circuits Conf.*, 2001, pp. 229–232.

[2] A. Asenov, S. Kaya, and J. H. Davies, "Intrinsic threshold voltage fluctuations in decanano MOSFETs due to local oxide thickness variations," *IEEE Trans. Electron Devices*, vol. 49, no. 1, pp. 112–119, Jan. 2002.

[3] A. Asenov, G. Slavcheva, A. R. Brown, J. Davies, and S. Saini, "Increase in the random dopant induced threshold fluctuations and lowering in sub-100 nm MOSFETs due to quantum effects: A 3-D density-gradient simulation study," *IEEE Trans. Electron Devices*, vol. 48, no. 4, pp. 722–729, Apr. 2001.

[4] T. Mizuno, J. Okamura, and A. Toriumi, "Experimental study of threshold voltage fluctuation due to statistical variation of channel dopant number in MOSFET's," *IEEE Trans. Electron Devices*, vol. 41, no. 11, pp. 2216–2221, Nov. 1994.

[5] J. A. Croon, G. Storms, S. Winkelmeier, and I. Pollentier, "Line-edge roughness: Characterization, modeling, and impact on device behavior," in *Proc. IEEE Int. Electronic Devices Meeting*, 2002, pp. 307–310.

[6] M. Pelgrom, A. Duinmaijer, and A. Welbers, "Matching properties of MOS transistors," *IEEE J. Solid-State Circuits*, vol. 24, no. 5, pp. 1433–1439, Oct. 1989.

[7] C. Michael and M. Ismail, *Statistical Modeling for Computer-Aided Design of MOS VLSI Circuits*. Boston, MA: Kluwer, 1993.

[8] H. Zhang, Y. Zhao, and A. Doboli, "ALAMO: An improved σ-space based methodology for modeling process parameter variations in analog circuits," in *Proc. IEEE Design, Autom. Test Eur. Conf.*, 2006, pp. 156–161.

[9] P. R. Gray and R. G. Meyer, *Analysis and Design of Analog Integrated Circuits*. New York: Wiley, 1984.

[10] A. Demir, E. Liu, and A. S-Vincentelli, "Time-domain non-Monte Carlo noise simulation for nonlinear dynamic circuits with arbitrary excitations," in *Proc. IEEE/ACM Int. Conf. Comput.-Aided Des.*, 1994, pp. 598–603.

[11] N. H. Hamid, A. F. Murray, and S. Roy, "Time-domain modeling of low-frequency noise in deep-submicrometer MOSFET," *IEEE Trans. Circuits Syst I, Reg. Papers*, vol. 55, no. 1, pp. 245–257, Jan. 2008.

[12] A. Dastgheib and B. Murmann, "Calculation of total integrated noise in analog circuits," *IEEE Trans. Circuits Syst I, Reg. Papers*, vol. 55, no. 10, pp. 2988–2993, Oct. 2008.

[13] R. López-Ahumada and R. R-Macías, "FASTEST: A tool for a complete and efficient statistical evaluation of analog circuits. DC analysis," *Analog Integr. Circuits Signal Process.*, vol. 29, no. 3, pp. 201–212, 2001.

[14] G. Biagetti, S. Orcioni, C. Turchetti, P. Crippa, and M. Alessandrini, "Sisma-a statistical simulator for mismatch analysis of MOS ICs," in *Proc. IEEE/ACM Int. Conf. Comput.-Aided Des.*, 2002, pp. 490–496.

[15] B. De Smedt and G. Gielen, "WATSON: Design space boundary exploration and model generation for analogue and RF IC design," *IEEE Trans. Comput.-Aided Des. Integr. Circuits Syst.*, vol. 22, no. 2, pp. 213–224, Feb. 2003.

[16] B. Linares-Barranco and T. S-Gotarredona, "On an efficient CAD implementation of the distance term in pelgrom's mismatch model," *IEEE Trans. Comput.-Aided Des. Integr. Circuits Syst.*, vol. 26, no. 8, pp. 1534–1538, Aug. 2007.

[17] J. Kim, J. Ren, and M. A. Horowitz, "Stochastic steady-state and AC analyses of mixed-signal systems," in *Proc. IEEE Design Autom. Conf.*, 2009, pp. 376–381.

[18] A. Zjajo and J. P. de Gyvez, "Analog automatic test pattern generation for quasi-static structural test," *IEEE Trans. Very Large Scale Integr. (VLSI) Syst.*, vol. 17, no. 10, pp. 1383–1391, Oct. 2009.

[19] J. Roychowdhury, "Reduced-order modeling of time-varying systems," *IEEE Trans. Circuits Syst. II, Analog Digit. Signal Process.*, vol. 46, no. 10, pp. 1273–1288, Oct. 1999.

[20] V. Vasudevan, "A time-domain technique for computation of noise-spectral density in linear and nonlinear time-varying circuits," *IEEE Trans. Circuits Syst I, Reg. Papers*, vol. 51, no. 2, pp. 422–433, Feb. 2004.

[21] N. Mi, J. Fan, S. X.-D. Tan, Y. Cai, and X. Hong, "Statistical analysis of on-chip power delivery networks considering lognormal leakage current variations with spatial correlation," *IEEE Trans. Circuits Syst I, Reg. Papers*, vol. 55, no. 7, pp. 2064–2075, Jul. 2008.

[22] E. Felt, S. Zanella, C. Guardiani, and A. Sangiovanni-Vincentelli, "Hierarchical statistical characterization of mixed-signal circuits using behavioral modeling," in *Proc. IEEE/ACM IC Comput.-Aided Des.*, 1996, pp. 374–380.

[23] M. Grigoriu, "On the spectral representation method in simulation," *Probabilistic Eng. Mech.*, vol. 8, pp. 75–90, 1993.

[24] M. Loève, *Probability Theory*. New York: Van Nostrand, 1960.

[25] R. Ghanem and P. D. Spanos, *Stochastic Finite Element: A Spectral Approach*. New York: Springer, 1991.

[26] J. Xiong, V. Zolotov, and L. He, "Robust extraction of spatial correlation," in *Proc. IEEE Int. Symp. Phys. Des.*, 2006, pp. 2–9.

[27] J. Vlach and K. Singhal, *Computer Methods for Circuit Analysis and Design*. New York: Van Nostrand Reinhold, 1983.

[28] L. O. Chua, C. A. Desoer, and E. S. Kuh, *Linear and Nonlinear Circuits*. New York: McGraw-Hill, 1987.

[29] L. Arnold, *Stochastic Differential Equations: Theory and Application*. New York: Wiley, 1974.

[30] A. Sangiovanni-Vincentelli, "Circuit simulation" in computer design aids for VLSI circuits," in *Computer Design Aids for VLSI Circuits*. Alphen aan den Rijn, The Netherlands: Sijthoff & Noordhoff, 1980.

[31] P. Heydari and M. Pedram, "Model-order reduction using variational balanced truncation with spectral shaping," *IEEE Trans. Circuits Syst I, Reg. Papers*, vol. 53, no. 4, pp. 879–891, Apr. 2006.

[32] M. D. Marco, M. Forti, M. Grazzini, P. Nistri, and L. Pancioni, "Lyapunov method and convergence of the full-range model of CNNs," *IEEE Trans. Circuits Syst I, Reg. Papers*, vol. 55, no. 11, pp. 3528–3541, Nov. 2008.

[33] K. H. Lim, K. P. Seng, L.-M. Ang, and S. W. Chin, "Lyapunov theory-based multilayered neural network," *IEEE Trans. Circuits Syst. II, Exp. Briefs*, vol. 56, no. 4, pp. 305–309, Apr. 2009.

[34] X. Liu, "Stability analysis of switched positive systems: A switched linear copositive Lyapunov function method," *IEEE Trans. Circuits Syst. II, Exp. Briefs*, vol. 56, no. 5, pp. 414–418, May 2009.

[35] R. H. Bartels and G. W. Stewart, "Solution of the matrix equation $AX + XB = C$," *Commun. Assoc. Comput. Mach.*, vol. 15, pp. 820–826, 1972.

[36] N. J. Higham, "Perturbation theory and backward error for $AX - XB = C$," *BIT Numer. Math.*, vol. 33, pp. 124–136, 1993.

[37] T. Penzl, "Numerical solution of generalized Lyapunov equations," *Adv. Comput. Math.*, vol. 8, pp. 33–48, 1998.

[38] G. H. Golub and C. F. van Loan, *Matrix Computations*. Baltimore, MD: Johns Hopkins Univ. Press, 1996.

[39] P. Benner and E. Quintana-Orti, "Solving stable generalized Lyapunov equations with the matrix sign function," *Numer. Algebra*, vol. 20, pp. 75–100, 1999.

[40] I. Jaimoukha and E. Kasenally, "Krylov subspace methods for solving large Lyapunov equations," *SIAM J. Numer. Anal.*, vol. 31, pp. 227–251, 1994.

[41] E. Wachspress, "Iterative solution of the Lyapunov matrix equation," *Appl. Math. Lett.*, vol. 1, pp. 87–90, 1998.

[42] J. Li, F. Wang, and J. White, "An efficient Lyapunov equation-based approach for generating reduced-order models of interconnect," in *Proc. IEEE/ACM Design Autom. Conf.*, 1999, pp. 1–6.

[43] T. L. Chen and G. Gildenblat, "Symmetric bulk charge linearisation in charge-sheet MOSFET model," *IEEE Electron. Lett.*, vol. 37, no. 12, pp. 791–793, Jun. 2001.

[44] R. van Langevelde, A. J. Scholten, and D. B. M. Klassen, Mos Model 11: Level 1102 Philips Res. Tech. Rep. 2004/85 [Online]. Available: http://www.nxp.com/models/mos_models/model11/

[45] A. Zjajo and M. Song, "Digitally programmable continuous-time bi-quad filter in 65-nm CMOs," in *Proc. IEEE Int. Symp. Radio-Frequency Integr. Technol.*, 2009, pp. 339–342.

[46] The numerics in control network NICONET [Online]. Available: http://www.win.tue.nl/wgs/niconet.html

Amir Zjajo (M'02) received the M.Sc. and DIC degrees from the Imperial College London, London, U.K., in 2000 and the Ph.D. degree from Eindhoven University of Technology, Eindhoven, The Netherlands in 2010, all in electrical engineering.

In 2000, he joined Philips Research Laboratories as a member of the research staff in the Mixed-Signal Circuits and Systems Group. From 2006 until 2009, he was with Corporate Research of NXP Semiconductors as a Senior Research Scientist. In 2009, he joined Delft University of Technology, Delft, The Netherlands, as a Faculty Member in the Circuit and Systems Group. He has published more than 30 papers in referenced journals and conference proceedings, and holds 3 patents with 7 more pending. He is the author *Low-Voltage High-Resolution A/D Converters: Design and Calibration* (Springer, 2010). His research interests include mixed-signal circuit design, signal integrity and timing, and yield optimization of VLSI.

Dr. Zjajo serves as a member of the Technical Program Committee of IEEE Design, Automation and Test in Europe Conference, and IEEE International Mixed-Signal Circuits, Sensors and Systems Workshop.
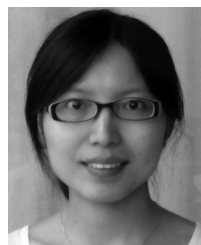
Qin Tang received the B.Sc. degree in the Department of Electronic Engineering, Southeast University, Nanjing, China, and the M.Sc. degree in the Department of Microelectronics and Solid State Electronics, School of Electronic Science and Engineering, Southeast University, in 2006 and 2008, respectively. She is currently working toward the Ph.D. degree in the Circuits and Systems group, Department of Microelectronics and Computer Engineering, Delft University of Technology, Delft, The Netherlands.

Her research interests include the analysis of process variations, gate modeling for timing analysis, and statistical static timing analysis.

Michel Berkelaar (M'96) received the M.Sc. and Ph.D. degrees in electrical engineering from Eindhoven University of Technology, Eindhoven. The Netherlands, in 1987 and 1992 respectively.

From 1992 to 2000 he was Assistant and Associate Professor at Eindhoven University of Technology. From 2000 to 2009 he was Director of Research at Magma Design Automation, Eindhoven. Currently, he is Project Leader for the European ENIAC MODERN project at Delft University of Technology, Delft, The Netherlands. He has published more than 50 papers at conferences and in journals, mainly in the areas of logic synthesis and statistical timing.

Dr. Berkelaar is an active reviewer and occasional topic chair for Design Automation and Test Europe (DATE), the International Conference on Computer-Aided Design (ICCAD), and the International Workshop on Logic and Synthesis (IWLS). For the latter he has also served as program chair.

José Pineda de Gyvez (F'09) received the Ph.D. degree from the Eindhoven University of Technology, Eindhoven, The Netherlands, in 1991.

From 1991 to 1999 he was a Faculty Member in the Department of Electrical Engineering, Texas A&M University. He was a Principal Scientist at Philips Research Laboratories, The Netherlands, from 1999 to 2006. He is currently a Senior Principal at NXP Semiconductors, Eindhoven. Since 2006 he also holds the professorship "Deep Submicron Integration" in the Department of Electrical Engineering at the Eindhoven University of Technology. He has more than 100 combined publications in the fields of testing, nonlinear circuits, and low power design. He is author or coauthor of three books, and has a number of granted patents.

Dr. Pineda de Gyvez has been Associate Editor in IEEE TRANSACTIONS ON CIRCUITS AND SYSTEMS— PART I: REGULAR PAPERS and TRANSACTIONS ON CIRCUITS AND SYSTEMS—PART II: EXPRESS BRIEFS, and also Associate Editor for Technology in IEEE TRANSACTIONS ON SEMICONDUCTOR MANUFACTURING. He is also a member of the editorial board of the *Journal of Low Power Electronics*. His work has been acknowledged in academic environments as well as in patent portfolios of many companies. His research has been funded by the Dutch Ministry of Science, U.S. Office of Naval Research, and U.S. National Science Foundation, among others.

Alessandro Di Bucchianico received the M.Sc. degree in mathematics from Amsterdam University, The Netherlands, and the Ph.D. degree in mathematics from Groningen University, The Netherlands.

Currently he is Associate Professor of Statistics at the Mathematics and Computing Science Department of the Eindhoven University of Technology, Eindhoven, The Netherlands, and Deputy Head of the Laboratory of Industrial Mathematics Eindhoven. As of 2007, he is also Director of the Permanent Office of ENBIS, the European Network of Business and Industrial Statistics. He has published over 30 papers in international journals on a wide range of topics in both applied and theoretical statistics. His main research interests are statistical process control, reliability (both hardware software reliability), experimental design, and statistical software.

Dr. Di Bucchianico was one of the coordinators of the Industrial Statistics programme at the European research institute EURANDOM from 1999 to 2009. From 1996 to 2001 he served on the board of the Mathematical Statistics Section of the Dutch Society for Statistics and Operations Research. He is a member of the BETA Research school for Operations Management and Logistics as well of the Stieltjes Institute for Mathematics. He is an associate editor of Quality and Reliability Engineering International and Statistica Neerlandica.

Nick van der Meijs (M'87) received the M.Sc and Ph.D degrees from Delft University of Technology, Delft, The Netherlands, in 1985 and 1992 respectively.

Currently, he is an Associate Professor at the Delft University of Technology in the Circuits and Systems group of the Department of Micro Electronics and Computer Engineering. As a Director of Studies he is responsible for the content, organization and quality of the B.Sc. and M.Sc. curricula in electrical engineering and computer engineering at TU Delft. He has authored or coauthored some 100 papers on various topics including design frameworks, interconnect optimization, and parasitics modeling, and was one of the lead developers of the SPACE 2D and 3D parasitic layout to circuit extractor. He is a regular reviewer for various EDA and design methodology conferences and journals, and has served as topic chair on multiple at conferences. He and his research group currently work both on modeling of parasitic effects in advanced integrated circuits and on circuit level design methods and tools for dealing with variability.